Silicon Nitride Inactivates SARS-CoV-2 *in vitro*

Caitlin W. Lehman[1,2], Rafaela Flur[1,2], Kylene Kehn-Hall, PhD[1,2], Bryan J. McEntire, PhD. MBA[3], B. Sonny Bal, MD, PhD, JD, MBA[3], and Ryan M. Bock, PhD[3]*

[1]Department of Biomedical Sciences and Pathobiology, Virginia Polytechnic Institute and State University, 1981 Kraft Drive, Blacksburg, VA 24060; [2]National Center for Biodefense and Infectious Diseases, School of Systems Biology, George Mason University, 10650 Pyramid Place, MS 1J5, Manassas, VA 20110; [3]SINTX Technologies, Inc., 1885 W. 2100 S. Salt Lake City, UT 84119.

ABSTRACT

Introduction

Severe acute respiratory syndrome coronavirus 2 (SARS-CoV-2), which is responsible for the COVID-19 pandemic, remains viable and therefore potentially infectious on several materials. One strategy to discourage the fomite-mediated spread of COVID-19 is the development of materials whose surface chemistry can spontaneously inactivate SARS-CoV-2. Silicon nitride (Si_3N_4), a material used in spine fusion surgery, is one such candidate because it has been shown to inactivate several bacterial species and viral strains. This study hypothesized that contact with Si_3N_4 would inactivate SARS-CoV-2, while mammalian cells would remain unaffected.

Materials

SARS-CoV-2 virions ($2x10^4$ PFU/mL diluted in growth media) were exposed to 5, 10, 15, and 20% (w/v) of an aqueous suspension of sintered Si_3N_4 particles for durations of 1, 5, and 10 minutes, respectively. Before exposure to the virus, cytotoxicity testing of Si_3N_4 alone was assessed in Vero cells at 24 and 48 hour post-exposure times. Following each exposure to Si_3N_4, the remaining infectious virus was quantitated by plaque assay.

Results

Vero cell viability increased at 5% and 10% (w/v) concentrations of Si_3N_4 at exposure times up to 10 minutes, and there was only minimal impact on cell health and viability up to 20% (w/v). However, the SARS-CoV-2 titers were markedly reduced when exposed to all concentrations of Si_3N_4; the reduction in viral titers was between 85% - 99.6%, depending on the dose and duration of exposure.

Conclusions

Si_3N_4 was non-toxic to the Vero cells while showing strong antiviral activity against SARS-CoV-2. The viricidal effect increased with increasing concentrations of Si_3N_4 and longer duration of exposure. Surface treatment strategies based on Si_3N_4 may offer novel methods to discourage SARS-CoV-2 persistence and infectivity on surfaces and discourage the spread of COVID-19.

*Corresponding Author: Ryan M. Bock, Email: RBock@sintx.com; Phone: 801-839-3551.

Keywords: Virus, Silicon Nitride, COVID-19, SARS-CoV-2, Nitrogen.

1. INTRODUCTION.

The spread of viruses through contaminated surfaces is of concern in crowded indoor environments such as schools, nursing homes, hospitals, and day-care centers.[1] In addition to the aerosol transmission of respiratory viruses due to sneezing, coughing, and talking, evidence suggests that contaminated hands and fomites also play a significant role in the person-to-person proliferation of disease.[2] The global spread of COVID-19, the disease caused by the coronavirus designated as SARS-CoV-2, has rekindled interest in the role of contaminated surfaces in viral transmission.

Viruses can survive for long periods on a variety of surfaces. Rotavirus is the agent that causes acute diarrhea in pediatric patients. In fecal samples, rotavirus particles are stable even after 2½ months of storage at temperatures above 30˚C, with even longer survival times at lower temperatures.[3] The 2002 outbreak of severe acute respiratory syndrome (SARS) in China was caused by SARS-CoV;[4, 5] a virus that is infective for up to 9 days in suspension, and 6 days in the dried state.[6] The pathogenic coronavirus HuCoV-229E causes upper respiratory infections in humans; at room temperature, this virus can persist for up to 5 days on surfaces ranging from glass to stainless steel.[7] A recent report has shown survival times of 4 to 72 hours of SARS-CoV-2 on plastic, copper, and cardboard surfaces, and up to 7 days on surgical masks.[8]

Surface decontamination by disinfectant application,[9] or by irradiation,[10, 11] can control fomite-induced viral spread. Some materials, notably metals such as copper (Cu), zinc (Zn), iron (Fe), and silver (Ag) have also been shown to rapidly inactivate viruses, including SARS-CoV-2.[7, 12, 13] Incorporation of Cu alloy surfaces in health care facilities reduces the microbial burden and the incidence of nosocomial infections.[14–16] Quaternary ammonium compounds such as ammonium chloride are also capable of inactivating viruses by deactivating the protective lipid coating that envelopes viruses like SARS-CoV-2 rely on; these compounds are used as disinfectants to clean surfaces and remove persistent viral particles.[17]

Silicon nitride (Si_3N_4) is a non-oxide ceramic that is FDA-cleared for use in implantable spinal fusion devices; clinical data have shown excellent long-term outcomes in both lumbar and cervical fusion with Si_3N_4 when compared to other spine biomaterials such as bone grafts, titanium, and polyetheretherketone.[18–23] In aqueous environments, Si_3N_4 spine implants undergo surface hydrolysis, resulting in the microscopic elution of ammonia which is converted into ammonium, nitrous oxide, and other reactive nitrogen species that inhibit bacterial growth and proliferation.[24] This inherent resistance to bacterial colonization may explain the lower incidence of bacterial infection with Si_3N_4 spinal implants (< 0.006%) when compared to other spine biomaterials (2.7% to 18%).[25]

Similar to bacterial inhibition, viral exposure to an aqueous solution of Si_3N_4 particles inactivated H1N1 (Influenza A/Puerto Rico/8/1934), Enterovirus (EV-A71), and Feline calicivirus.[26] Recent findings have shown that Si_3N_4 particles in aqueous suspensions also inactivated SARS-CoV-2 with antiviral activity that compared favorably to Cu ions. Unlike Si_3N_4, Cu exhibited toxicity to mammalian cells.[12] The present study hypothesized that exposure to Si_3N_4 would not elicit a toxic response from mammalian cells under experimental conditions while demonstrating a time- and dose-dependent inactivation of SARS-CoV-2.

2. MATERIALS AND METHODS.

2.1. Preparation of Si_3N_4 powder.

A doped Si_3N_4 powder (SINTX Technologies, Inc., Salt Lake City, UT USA) with a nominal composition of 90 wt.% α-Si_3N_4, 6 wt.% yttria (Y_2O_3), and 4 wt.% alumina (Al_2O_3) was prepared by aqueous mixing and spray-drying of the inorganic constituents, followed by sintering of the spray-dried granules (~1700°C for ~3 h), hot-isostatic pressing (~1600°C, 2 h, 140 MPa in N_2), aqueous-based comminution, and freeze-drying.[27] The resulting powder had a trimodal distribution with an average particle size of 0.8 ± 1.0 µm as shown in Figure 1. Doping Si_3N_4 with Y_2O_3 and Al_2O_3 is essential to densify the ceramic and convert it from its α- to ß-phase during sintering. The mechanism of densification is via dissolution of α-phase and subsequent precipitation of ß-phase grains facilitated by the formation of a transient intergranular liquid that solidifies during cooling. ß-Si_3N_4 is therefore a composite composed of about 10 wt.% intergranular glass phase (IGP) and 90 wt.% crystalline ß-Si_3N_4 grains.

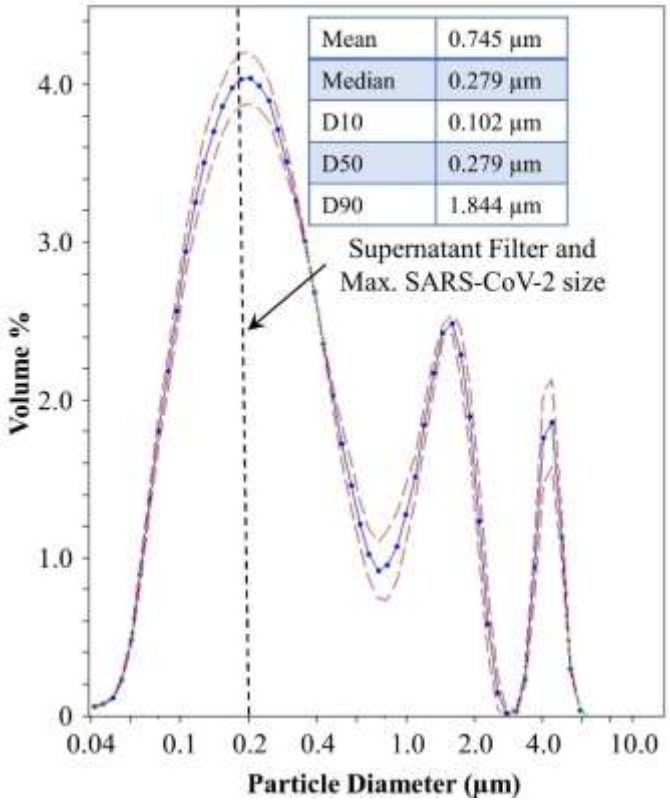

Figure 1. Silicon nitride powder particle size distribution.

2.2. Cell culture and viral stocks.

Vero green African monkey kidney epithelial cells (ATCC, Cat #CCL-81) were chosen for this analysis due to their ability to support high levels of SARS-CoV-2 replication and their use in antiviral testing.[28, 29] These cells were cultured in DMEM (VWR, Cat # 10128-206) supplemented with 10% FBS (VWR Cat # 97068-085), 1% L-glutamine (VWR Cat # 45000-676), and 1% penicillin/streptomycin (VWR Cat # 45000-652). Cells were maintained at 37°C and 5% CO_2. SARS-CoV-2 isolate USA-WA1/2020 was obtained from BEI Resources (Cat #NR-52281). Vero cells were inoculated with SARS-CoV-2 (MOI 0.1) to generate viral stocks. Cell-free supernatants were collected at 72 hours post-infection and clarified via

centrifugation at 10,000 rpm for 10 minutes and filtered through a 0.2 µm filter (Pall, Cat # 4433). Stock virus was titered according to the plaque assay protocol detailed below.

2.3. Cell viability assays.

The Si_3N_4 powder was suspended in 1 mL DMEM growth media in microcentrifuge tubes. Tubes were vortexed for 30 seconds to ensure adequate contact and then placed on a tube revolver for either 1, 5, or 10 minutes. At each time point, the samples were centrifuged, and the supernatant was collected and filtered through a 0.2 µm filter. Clarified supernatants were added to cells for either 24 or 48 hours. Untreated cells were maintained alongside as controls. Cells were tested at each time point using CellTiter Glo (Promega, Cat #G7570), which measures ATP production, to determine cell viability.

2.4. Antiviral activity testing.

SARS-CoV-2 was diluted in DMEM growth media to a concentration of 2×10^4 PFU/mL. Four mL of the diluted virus was added to tubes containing silicon nitride at 20, 15, 10, and 5% (w/v). The virus without Si_3N_4 was processed in parallel as a control. Tubes were vortexed for 30 seconds to ensure adequate contact and then placed on a tube revolver for either 1, 5, or 10 minutes, while a virus only control was incubated for the maximum 10 minutes. At each time point, the samples were centrifuged, and the supernatant was collected and filtered through a 0.2 µm filter. The remaining infectious virus in the clarified supernatant was quantitated by plaque assay. An overview of the antiviral testing method is provided in Figure 2.

2.5. SARS-CoV-2 plaque assay.

Vero cells were plated at 2×10^5 cells/well in a 12-well plate on the day before the plaque assay. Clarified supernatants from the antiviral testing were serially diluted (10-fold) and 200 µL was added to Vero cells which were incubated for 1 hour at 37°C, 5% CO_2. Plates were rocked every 15 minutes to ensure adequate coverage and at 1 hour, a 1:1 ratio of 0.6% agarose and 2X EMEM (VWR, Cat # 10128-758) supplemented with 5% FBS, 2% penicillin/streptomycin, 1% non-essential amino acids (VWR, Cat # 45000-700), 1% sodium pyruvate (VWR, Cat # 45000-710), and 1% L-glutamine was added to the cells before incubating for 48 hours at 37°C, 5% CO_2. After incubation, the cells were fixed with 10% formaldehyde and stained with 2% crystal violet in 20% ethanol for counting.

3. RESULTS

3.1. No toxicity of Si_3N_4 to Vero cells up to 20 wt.%/vol.

The impact of Si_3N_4 on eukaryotic cell viability was tested. Si_3N_4 was resuspended in cell culture media at 5, 10, 15, and 20% (w/v). Samples were collected at 1, 5, and 10 minutes and added to Vero cells. Vero cell viability was measured at 24 and 48 hours post-exposure (Figure 3A and 3B). No significant decrease in cell viability was observed at either 24 or 48 hours post-exposure with 5%, 10%, or 15% silicon nitride. A small impact on cell viability (~10% decrease) was observed at 48 hours in cells exposed to 20% Si_3N_4. Interestingly, a ~10% increase in Vero cell viability was observed at 48 hours with the 5% - 10 minute and 10% - 10 minute samples (Figure 3B), suggesting that Si_3N_4 may be stimulating cell growth or cellular metabolism under these conditions. These data indicate that Si_3N_4 has minimal impact on Vero cell health and viability up to 20 wt.%/vol.

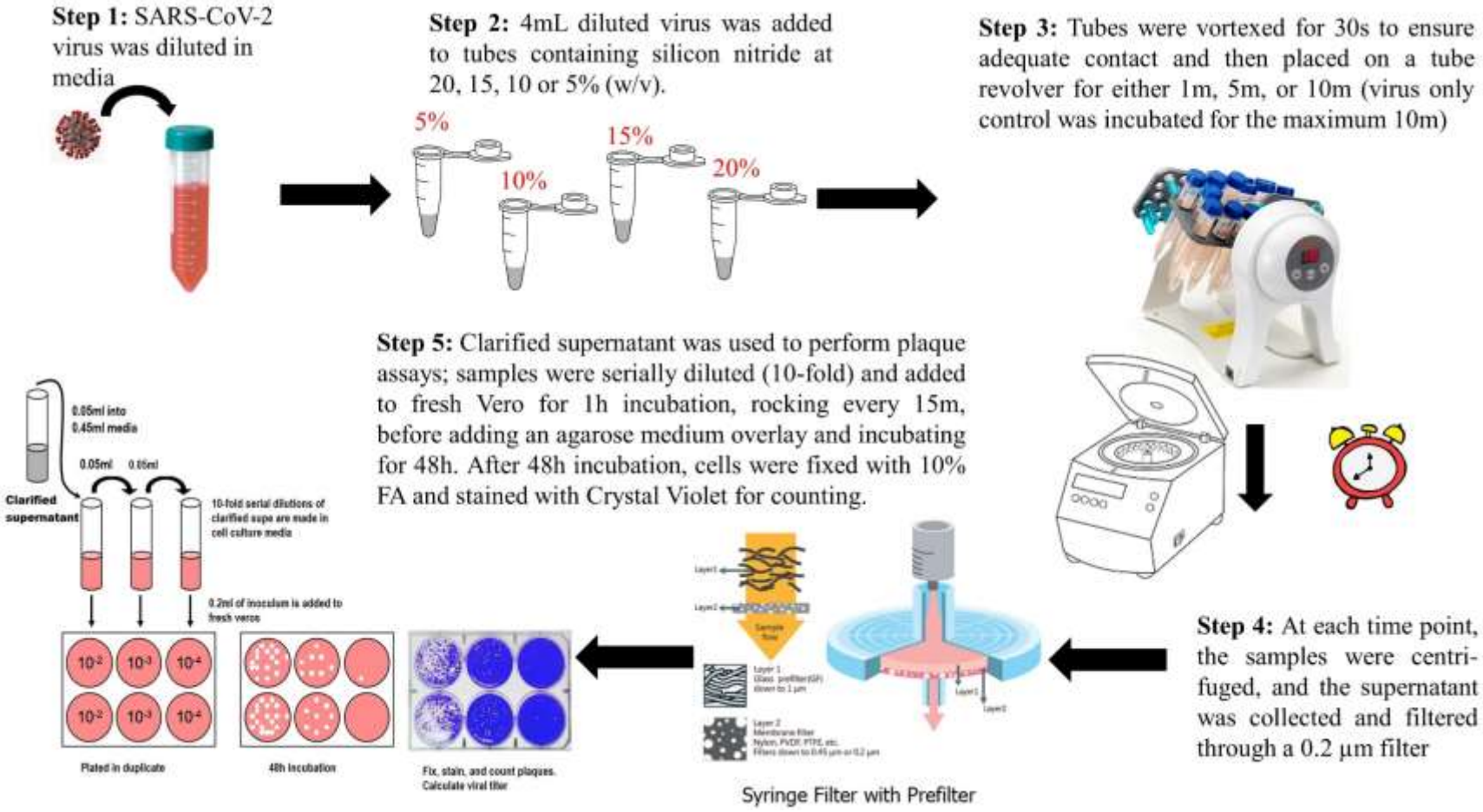

Figure 2. A Pictorial overview of the antiviral testing method.

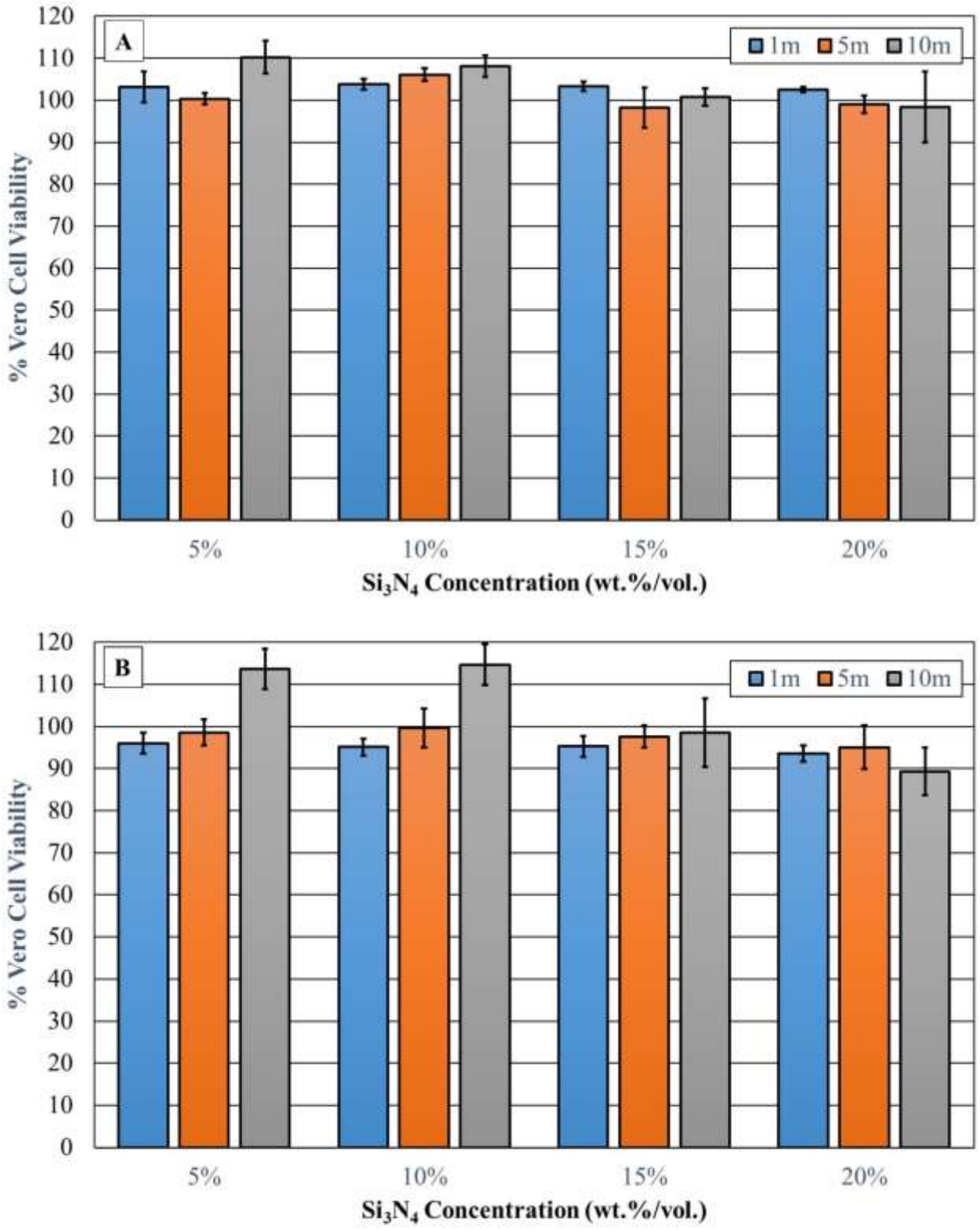

Figure 3. Cytotoxicity testing of silicon nitride. Silicon nitride at concentrations of either 5, 10, 15 or 20 wt.%/vol (n=4) were incubated with cell culture media for 1, 5, and 10m. At each timepoint, the samples were centrifuged, and the supernatant was collected and filtered through a 0.2um filter. The clarified supernatant was added to Vero cells and their viability assessed at 24 h (A) and 48 h (B). Untreated Vero cells served as a control and were set to 100% viability.

3.2. Si_3N_4 Inactivated SARS-CoV-2.

Given that 5, 10, 15, and 20% Si_3N_4 were non-toxic to Vero cells, antiviral testing at these concentrations was performed. SARS-CoV-2 virions were exposed to Si_3N_4 at these concentrations for 1, 5, or 10 minutes. Following Si_3N_4 exposure, the infectious virus remaining in each solution was determined through plaque assay. Virus processed in parallel but only exposed to cell culture media contained 4.2 x 10^3 PFU/mL. SARS-CoV-2 titers were reduced when exposed to all concentrations of Si_3N_4 tested (Figures 4A and B). The inhibition was dose-dependent with SARS-CoV-2 exposed for 1 minute and 5% Si_3N_4 having reduced viral titers by ~0.8 $\log_{10}$, 10% Si_3N_4 by ~1.2 $\log_{10}$, 15% Si_3N_4 by 1.4 $\log_{10}$, and 20% Si_3N_4 by 1.7 $\log_{10}$ (Figure 4A). Similar results were observed with the 5 and 10 minute samples. This reduction in viral titers corresponded to 85% viral inhibition at 5% Si_3N_4, 93% at 10% Si_3N_4, 96% at 15% Si_3N_4, and 98% viral inhibition at 20% Si_3N_4 (Figure 4B). Higher Si_3N_4 concentrations for longer times resulted in increased inhibition – leading to 99.6% viral inhibition at 20% Si_3N_4 and 10 minute exposure (Figure 4B). These data indicate that Si_3N_4 has a strong antiviral effect against SARS-CoV-2.

4. DISCUSSION

The remarkable finding in the present study is that a one-minute exposure to a 5% solution of Si_3N_4 resulted in 85% inactivation of SARS-CoV-2, while Vero cell viability was minimally impacted even after a 48 hour exposure to a 20% concentration of the same material. This finding is consistent with previous work showing that Si_3N_4 exerts a fortuitous dual effect, whereby the material can inactivate viruses[12, 26] and inhibit bacterial biofilm formation[29] without negatively impacting mammalian cell viability. The present study is also consistent with a recent investigation that showed the rapid inactivation of SARS-CoV-2 upon exposure to 15% (w/v) Si_3N_4,[12] and related data showing that the antiviral effect of Si_3N_4 may be generally applicable to other single-strand RNA viruses such as Influenza A, Feline calicivirus, and Enterovirus.[26] Taken together, these studies suggest that Si_3N_4 may be a suitable material platform for the development of fabrics for personal protective equipment such as masks, and also to manufacture commonly-touched surfaces where viral persistence may encourage the spread of disease.

The antiviral effect of Si_3N_4 is related to several probable mechanisms that have been hypothesized previously.[12] One mechanism is the viral RNA fragmentation by reactive nitrogen species derived from a slow and controlled elution of ammonia from the surface of Si_3N_4; and the subsequent formation of ammonium, with the release of free electrons and negatively charged silanols in aqueous solution. Also, as reported previously, the similarity between the protonated amino groups, $Si–NH_3^+$ at the surface of Si_3N_4 and the N-terminal of lysine, $C–NH_3^+$ on the virus triggers a competitive binding that leads to SARS-CoV-2 inactivation.[12] An advantage of Si_3N_4 is that these phenomena reflect a sustained mechanism of action secondary to a hydrolysis-mediated chemical equilibrium on the surface of the material, rather than a reliance on repeated applications required of commonly-used disinfecting agents.

While the antiviral effectiveness of Si_3N_4 is comparable to Cu, a historically-recognized viricidal agent, the use of Cu is limited by its cell toxicity.[30] In contrast to Cu, ceramic implants made of Si_3N_4 that have the same composition as the material used in this study have shown successful clinical and radiographic outcomes even after three decades in the human body.[31] An advantage of Si_3N_4 toward the potential development of antiviral and antibacterial surfaces is the versatility of the material; thus sintered Si_3N_4 has been incorporated into polymers, bioactive glasses, and even other ceramics to create composites and coatings that retain the favorable osteogenic and antibacterial properties of Si_3N_4.[32–36]

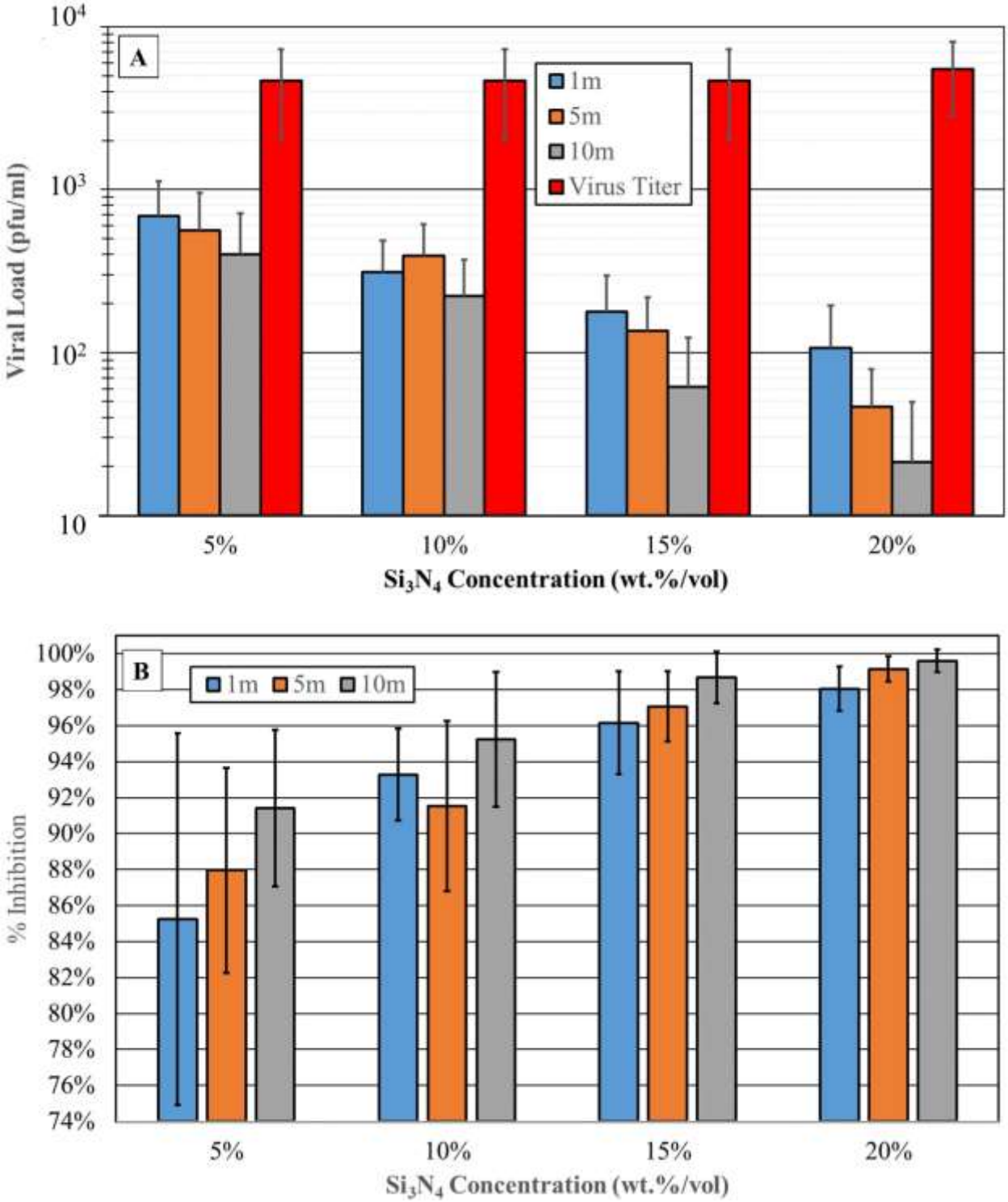

Figure 4. Silicon nitride antiviral activity testing. Silicon nitride at concentrations of 5, 10, 15, and 20 wt.%/vol were incubated with virus diluted in cell culture media for 1, 5, and 10m. At each timepoint, the samples were centrifuged, and the supernatant was collected and filtered through a 0.2um filter. The clarified supernatant was used to perform plaque assay in duplicate (neat through -5 dilutions were plated); (A) Data are expressed as PFU/mL. N=4 (two biological replicates and two technical replicates); (B) Data are expressed as % inhibition, with the virus only control (media only) set to 0%.

We recognize that this study has limitations; a powdered form of doped-Si_3N_4 was used, rather than the monolithic material employed as spine implants. While this study demonstrates that this powdered form of doped-Si_3N_4 is an effective antiviral agent, future studies will need to show that its viricidal efficacy is retained when compounded into or coated onto other materials such as polymers, paints, metals, fabrics, or ceramics. To be truly effective, the surface hydrolysis and release kinetics of *ß*-Si_3N_4's moieties will have to be optimized for each composite material and device. Additionally, further refinement of the current composition of doped *ß*-Si_3N_4 may enhance its ability to release these moieties for the benefit of mammalian cells and the destruction of pathogens. Studies are also needed to identify whether simple physical contact with Si_3N_4 particles, or exposure to its soluble components, or both, are necessary for the antipathogenic effects observed in the present study.

5. CONCLUSIONS

In the present study, Si_3N_4 proved harmless to mammalian cells, while demonstrating a time- and dose-dependent inactivation of SARS-CoV-2. While Si_3N_4 is not suitable for ingestion or inhalation, its antiviral activity, which is not limited to SARS-CoV-2, suggests that it may be a fortuitous platform to engineer surfaces and personal protective equipment to discourage viral persistence, and thereby control the spread of COVID-19 and other diseases.

ACKNOWLEDGEMENT

The following reagent was deposited by the Centers for Disease Control and Prevention and obtained through BEI Resources, NIAID, NIH: SARS-Related Coronavirus 2, Isolate USA-WA1/2020, NR-52281.

CONFLICTS OF INTEREST

This study was supported by SINTX Technologies, Inc., (Salt Lake City, UT USA) of which Drs. Bryan J. McEntire, B. Sonny Bal, and Ryan M. Bock are either principals or employees. The other coauthors declare no conflicts of interest.

REFERENCES

1. Barker J, Stevens D, Bloomfield SF. Spread and Prevention of Some Common Viral Infections in Community Facilities and Domestic Homes. *J Appl Microbiol*. 2001;91(1):7–21.
2. Vasickova P, Pavlik I, Verani M, Carducci A. Issues Concerning Survival of Viruses on Surfaces. *Food Environ Virol*. 2010;2(1):24–34.
3. Fischer TK, Steinsland H, Valentiner-Branth P. Rotavirus Particles Can Survive Storage in Ambient Tropical Temperatures for More than 2 Months. *J Clin Microbiol*. 2002;40(12):4763–4764.
4. Drosten C, Günther S, Preiser W, *et al.* Identification of a Novel Coronavirus in Patients with Severe Acute Respiratory Syndrome. *N Engl J Med*. 2003;348(20):1967–1976.
5. Drosten C, Preiser W, Gunther S, Schmitz H, Doerr HW. Severe Acute Respiratory Syndrome: Identification of the Etiological Agent. *Trends Mol Med*. 2003;9(8):325–327.
6. Rabenau HF, Cinatl J, Morgenstern B, Bauer G, Preiser W, Doerr HW. Stability and Inactivation of SARS Coronavirus. *Med Microbiol Immunol*. 2005;194(1–2):1–6.
7. Warnes SL, Little ZR, Keevil CW. Human Coronavirus 229E Remains Infectious on Common Touch Surface Materials. *MBio*. 2015;6(6):1–10.
8. Chin A, Chu J, Perera M, *et al.* Stability of SARS-CoV-2 in Different Environmental Conditions. *Lancet Micorbe 2020*. 2020;5247(April 2, 2020):2020.03.15.20036673.
9. Rabenau HF, Kampf G, Cinatl J, Doerr HW. Efficacy of Various Disinfectants Against SARS Coronavirus. *J*

Hosp Infect. 2005;61(2):107–111.
10. Tseng CC, Li CS. Inactivation of Viruses on Surfaces by Ultraviolet Germicidal Irradiation. *J Occup Environ Hyg*. 2007;4(6):400–405.
11. Tseng CC, Li CS. Inactivation of Virus-Containing Aerosols by Ultraviolet Germicidal Irradiation. *Aerosol Sci Technol*. 2005;39(12):1136–1142.
12. Pezzotti G. Rapid Inactivation of SARS-CoV-2 by Silicon Nitride, Copper, and Aluminum Nitride. *bioRxiv Prepr*. 2020;1–16.
13. Sagripanti JL, Routson LB, Lytle CD. Virus Inactivation by Copper or Iron Ions Alone and in the Presence of Peroxide. *Appl Environ Microbiol*. 1993;59(12):4374–4376.
14. Karpanen TJ, Casey AL, Lambert PA, *et al.* The Antimicrobial Efficacy of Copper Alloy Furnishing in the Clinical Environment: A Crossover Study. *Infect Control Hosp Epidemiol*. 2012;33(1):3–9.
15. Salgado CD, Sepkowitz KA, John JF, *et al.* Copper Surfaces Reduce the Rate of Healthcare-Acquired Infections in the Intensive Care Unit. *Infect Control Hosp Epidemiol*. 2013;34(5):479–486.
16. Schmidt MG, Attaway HH, Sharpe PA, *et al.* Sustained Reduction of Microbial Burden on Common Hospital Surfaces through Introduction of Copper. *J Clin Microbiol*. 2012;50(7):2217–2223.
17. Baker N, Williams AJ, Tropsha A, Ekins S. Repurposing Quaternary Ammonium Compounds as Potential Treatments for COVID-19. *Pharm Res*. 2020;37(6):1–4.
18. Smith MW, Romano DR, McEntire BJ, Bal BS. A Single Center Retrospective Clinical Evaluation of Anterior Cervical Discectomy and Fusion Comparing Allograft Spacers to Silicon Nitride Cages. *J Spine Surg*. 2018;4(2):349–360.
19. Ball HT, McEntire BJ, Bal BS. Accelerated Cervical Fusion of Silicon Nitride versus PEEK Spacers: A Comparative Clinical Study. *J Spine*. 2017;6(6):1000396.
20. Arts MP, Wolfs JFC, Corbin TP. Porous Silicon Nitride Spacers versus PEEK Cages for Anterior Cervical Discectomy and Fusion: Clinical and Radiological Results of a Single-Blinded Randomized Controlled Trial. *Eur Spine J*. 2017;26(9):2372–2379.
21. Calvert GC, Huffmon III G V, Rambo Jr WM, Smith MW, McEntire BJ, Bal BS. Clinical Outcomes for Anterior Cervical Discectomy and Fusion with Silicon Nitride Spine Cages: A Multicenter Study. *J Spine Surg*. 2019;5(4):504–519.
22. Calvert GC, Huffmon GVBI, Rambo WMJ, Smith MW, McEntire BJ, Bal BS. Clinical Outcomes for Lumbar Fusion using Silicon Nitride versus other Biomaterials. *J Spine Surg*. 2020;6(1):33–48.
23. McEntire BJ, Maislin G, Bal BS. Two-Year Results of a Double-Blind Multicenter Randomized Controlled Non-Inferiority Trial of PEEK versus Silicon Nitride Spinal Fusion Cages in Patients with Symptomatic Degenerative Lumbar Disc Disorders. *J Spine Surg*. 2020; In Press.
24. Pezzotti G. Silicon Nitride: A Bioceramic with a Gift. *ACS Appl Mater Interfaces*. 2019;acsami.9b07997.
25. Bock RM, Jones EN, Ray DA, Bal BS, Pezzotti G, McEntire BJ. Bacteriostatic Behavior of Surface-Modulated Silicon Nitride in Comparison to Polyetheretherketone and Titanium. *J Biomed Mater Res Part A*. 2017;105(5):1521–1534.
26. Pezzotti G, Boschetto F, Ogitani E, *et al.* A Potent Solid-State Bioceramic Inactivator of ssRNA Viruses. *Sci Rep*. 2020; In Press.
27. McEntire BJ, Lakshminarayanan R, Thirugnanasambandam P, Seitz-Sampson J, Bock R, O'Brien D. Processing and Characterization of Silicon Nitride Bioceramics. *Bioceram Dev Appl*. 2016;6(1):1000093.
28. Matsuyama S, Nao N, Shirato K, *et al.* Enhanced Isolation of SARS-CoV-2 by TMPRSS2- Expressing Cells. *Proc Natl Acad Sci U S A*. 2020;117(13):7001–7003.
29. Harcourt J, Tamin A, Lu X, *et al.* Severe Acute Respiratory Syndrome Coronavirus 2 from Patient with Coronavirus Disease, United States. *Emerg Infect Dis*. 2020;26(6):1266–1273.
30. Grass G, Rensing C, Solioz M. Metallic Copper as an Antimicrobial Surface. *Appl Environ Microbiol*. 2011;77(5):1541–1547.
31. Mobbs RJ, Rao PJ, Phan K, *et al.* Anterior Lumbar Interbody Fusion Using Reaction Bonded Silicon Nitride Implants: Long Term Case Series of the First Synthetic ALIF Spacer Implanted in Humans. *World Neurosurg*. 2018;120:256–264.
32. Pezzotti G, Zhu W, Marin E, *et al.* Improved Bioactivity and Bacteriostasis of PEEK Polymers by Addition of Silicon Nitride Particles Giuseppe. *Proc Annu Meet Orthop Res Soc*. 2018;0775.
33. Marin E, Boschetto F, Zanocco M, *et al.* KUSA-A1 Mesenchymal Stem Cells Response to PEEK-Si_3N_4

Composites. *Mater Today Chem*. 2020;(xxxx):100316.
34. Marin E, Adachi T, Zanocco M, *et al.* Enhanced Bioactivity of Si3N4 through Trench-Patterning and Back-Filling with Bioglass®. *Mater Sci Eng C*. 2019;106(October 2018):110278.
35. Pezzotti G, Marin E, Zanocco M, *et al.* Osteogenic Enhancement of Zirconia-Toughened Alumina with Silicon Nitride and Bioglass®. *Ceramics*. 2019;2:554–567.
36. Zanocco M, Boschetto F, Zhu W, *et al.* 3D-Additive Deposition of an Antibacterial and Osteogenic Silicon Nitride Coating on Orthopaedic Titanium Substrate. *J Mech Behav Biomed Mater*. 2020;103:103557.
37. Herrmann M, Schilm J, Hermel W, Michaelis A. Corrosion Behavior of Silicon Nitride Ceramics in Aqueous Solutions. *J Ceram Soc Japan*. 2006;114(11):1069–1075.
38. Jurkić LM, Cepanec I, Pavelić SK, Pavelić K. Biological and Therapeutic Effects of Ortho-Silicic Acid and some Ortho-Silicic Acid-Releasing Compounds: New Perspectives for Therapy. *Nutr Metab (Lond)*. 2013;10(1):2.
39. Henstock JR, Canham LT, Anderson SI. Silicon: The Evolution of its Use in Biomaterials. *Acta Biomater*. 2015;11:17–26.
40. Augustine R, Dalvi YB, Yadu Nath VK, *et al.* Yttrium Oxide Nanoparticle Loaded Scaffolds with Enhanced Cell Adhesion and Vascularization for Tissue Engineering Applications. *Mater Sci Eng C*. 2019;103(February).
41. Pezzotti G, Bock RM, Adachi T, *et al.* Silicon Nitride Surface Chemistry: A Potent Regulator of Mesenchymal Progenitor Cell Activity in Bone Formation. *Appl Mater Today*. 2017;9:82–95.
42. Pacher P, Beckman JS, Liaudet L. Nitric Oxide and Peroxynitrite in Health and Disease. *Physiol Rev*. 2007;87(1):315–424.
43. Zanocco M, Marin E, Rondinella A, *et al.* The Role of Nitrogen Off-Stoichiometry in the Osteogenic Behavior of Silicon Nitride Bioceramics. *Mater Sci Eng C*. 2019;105:110053.
44. McEntire BJ, Bal BS, Pezzotti G. Antimicrobial Nitric Oxide Releasing Compounds and Scaffolds. *ASTM STP Sel Tech Pap*. 2020;(in press).